ISSN: 2687-8100

Archives in Biomedical Engineering & Biotechnology

DOI: 10.33552/ABEB.2022.07.000651

Iris Publishers

Review Article

Using Electroencephalographic Data to Map the Scalp Distribution of Electrostatic Energy

Richard W Montgomery, Leslie D Montgomery*

LDM associates, Director of Research and Development, 1764 Emory Street, San Jose, USA

***Corresponding author:** Leslie D Montgomery, LDM associates, Director of Research and Development, 1764 Emory Street, San Jose, CA 95126, USA.

Received Date: October 27, 2022

Published Date: November 07, 2022

Abstract

This paper describes how ERP energy density analysis and marginal cost-benefit analysis were combined to interpret the results of an investigation of mental exhaustion. Eleven subjects competed in performing computer-generated mental arithmetic tasks over a period lasting, in some cases, 2.5 hours. Assuming that brain resources are dynamically allocated, marginal cost-benefit analysis of optimal resource allocation was used to interpret longitudinal changes in these subjects' ERP energy density. It was possible to graphically track each subject through four phases: learning, boredom, motivation, and fatigue. Phase trajectories of this sort may be useful in human factors research.

The purpose of this paper is to describe the method in sufficient practical detail to facilitate its exploitation by other researchers. Section II reproduces the standard derivation of the underlying formulas. Section III describes how these are implemented through multiple regression analysis of the voltage data. Section IV describes how the whole procedure may be computerized. Section V presents a gallery of figures from various experiments to illustrate the usefulness of energy ERPs.

Keywords: Event Related Potentials; Electroencephalography; EEG; Energy Density; Laplacian; Brain Resource Allocation; Cognitive Function

Introduction

Conventional multielectrode electroencephalographic (EEG) records contain all the information necessary to map the energy density distribution of the scalp electrostatic field. EEG traces are records of voltage rather than energy fluctuations. They show the voltage difference between the scalp electrode and a body reference such as linked earlobes. But voltage is energy per unit charge. This means that EEG voltage data would be an indicator of the energy of the scalp electrical fields only if it could be assumed that the charge density at the electrode site remained constant. The charge distribution is, however, constantly changing due to the same electrical fields.

Recent developments in EEG technique make it possible to overcome this problem. It is now common record from 20 or more electrodes simultaneously. This makes it possible to use regression methods to estimate the shape of the 'voltage surface' over the scalp at each instant. From that, it is possible to infer the concurrent distribution of scalp charge density and then to calculate the energy of the electrical fields that produce the scalp voltage and charge patterns. One of the standard results of mathematical physics is that the charge density distribution in an electrical field is proportional to the (spatial) rate of change of the voltage gradient [1]. This relationship is known as Poisson's equation, i.e., that charge density is proportional to the Laplacian of the voltage surface:

$$\rho(x,y) = -\varepsilon \nabla^2 \varphi(x,y)$$

where:

ρ = charge density

φ = voltage

$\nabla^2 = -(\partial^2 \varphi / \partial x^2 + \partial^2 \varphi / \partial y^2)$

ε = permittivity coefficient.

Hjorth [2] and Nunez [3] (1989) described how Poisson's equation could be estimated from the Laplacian of interpolated scalp voltage EEG data. Their interest was focused, however, on the charge density distribution by itself. They explained that fluctuations in charge density might indicate locations of current flow into or out of the skull, and hence the sites of underlying current sinks or sources. A localized current sink would plausibly indicate, for example, depolarization of apical dendrites in groups of subjacent, radially oriented pyramidal cells due to excitatory post-synaptic potentials.

When, following Ohm's Law, the charge density estimate is combined with the original voltage data it is possible to derive the scalp distribution of electrical field energy. Poisson's equation is simply multiplied by voltage. Representing Energy density as U(x,y),

$U(x,y) = -\varepsilon \varphi \nabla^2 \varphi$.

Cortical energy density mapping in this manner appears to be a valuable means of tracking cortical activation during the performance of cognitive tasks under various experimental conditions. It has been applied to the study of cortical localization of mental arithmetic [4,5], to the study of dyslexia, to an investigation of the effects of therapeutic cooling on cognitive performance of multiple sclerosis patients, and to the effects of mental fatigue. The purpose of this paper is to describe the method in sufficient practical detail to facilitate its exploitation by other researchers. Section II reproduces the standard derivation of the underlying formulas. Section III describes how these are implemented through multiple regression analysis of the voltage data. Section IV describes how the whole procedure may be computerized. Section V presents a gallery of figures from various experiments to illustrate the usefulness of energy ERPs.

EEG voltage data will certainly continue to have utility. Clinicians depend upon their familiarity with such data for diagnostic interpretation. And there is a vast body of EEG research linking voltage ERP peaks with hypothesized locations and stages of sensory processing. Nonetheless, the energy distribution of the scalp electrical field is probably most directly correlated with the spatial pattern of cortical activation, especially in the sense of metabolic energy dissipation. (See Roland, 1993, for an extensive discussion of the relationship between metabolic energy and the activation of cortical fields, by which they mean localized assemblies of functionally specialized columns of cortical cells.)

The brain uses an enormous amount of energy, not only in cellular maintenance, but also in the maintenance of the ionic gradients that underlie neuronal excitability and in the synthesis of transmitter substances. As Cotman and McGaugh (1980) remind us "The brain is one of the most metabolically active tissues in the body. In man, for example, the brain uses 40 ml of oxygen per minute, so that the brain, which is only about 2% of the total body weight, accounts for almost 20% of the total resting body oxygen consumption!" As with other tissue, much of it is dissipated as heat [6]. But while the dissipation of energy as heat is common to all tissue, neural tissue has the additional feature of dissipating considerable energy in the form of electrical fields created by ionic gradients.

This is the fact that is exploited by Positron Emission Tomography (PET) and similar scanning techniques to identify cortical localization of various sensory-motor and cognitive functions by mapping sites of elevated metabolism. By transforming EEG data (particularly ERPs) to show energy-density distributions, EEG can be used in a similar manner. EEG is a far simpler procedure, and one that allows much more flexibility in experimental design.

Related Results from Mathematical Physics

This section reviews the standard results of electrostatic field theory and shows how they lead to an equation that relates scalp electrostatic energy density to the electrode voltage levels recorded by EEG. The first step is the derivation of Poisson's equation, which relates charge density to voltage. The scalp electrostatic field is a force field arising from the Coulomb attraction or repulsion of charged particles. The force between two charged particles is vector quantity. The following expression for this force vector, as a function of the magnitude of the two charges and the distance between them, is known as Coulomb's Law:

$F = k Q_o Q r / r^2$

The unit vector r is directed along the line between the two charges. The scale constant, k, has the value $1/4\pi\varepsilon$ in the MKAS system, where ε represents the permittivity of free space, equal to approximately 8.8542×10^{-12} farad / meter. In the CGS system k has the value of unity. This simplification will be used here.

Regarding one of the particles as a 'test charge' used to explore the electrostatic field, and normalizing force (expressing it as per unit of the magnitude of the test charge), leads to a vector function of location called electrical field intensity.

$E(x,y,z) = F(x,y,z) / Q_o$.

In practice, the force on an exploring test charge is the linear, superposed result of a vast number (n) of other charges:

$F(x,y,z) = \sum_i=1 \text{ to } n \; Q_o Q_i r_i / r_i^2$

where ri is the unit vector directed toward the i-th charge from the position, x,y,z. Therefore, the corresponding expression for field intensity is:

$E(x,y,z) = \sum_i=1 \text{ to } n \; Q_i r_i / r_i^2$.

Viewing the collection of individual charges as a 'smeared' continuum of charge, the summations may be replaced by volume integrals:

$E(x,y,z) = \iiint_v \rho r / r^2 \, dv$.

The symbol 'ρ 'represents the limiting value of charge per unit volume, as volume goes to zero, and is called 'charge density.' Our attention will be focused on ρ because an essential step in estimating the scalp energy distribution is to first estimate the charge distribution.

The following paragraphs explain how ρ is calculated from ordinary EEG voltage data. It is important to recognize that E is a vector field. In order to compute the charge and energy distributions from voltage data (all of which are scalar fields) is not necessary to first compute the vector field E. It will be seen that E serves only as an intermediate concept which facilitates the algebraic derivations for the relationship between voltage, charge, and energy.

Although measured by means of currents induced in a grounded external circuit, the quantity that is measured by EEG is the electrical potential (potential to do work) associated with the electrical force field. Potential (or "voltage") is a scalar function of position φ (x,y,z). Its relationship to the electrical field is expressed as follows, where the z-dimension has been omitted, reflecting the fact that EEG pertains to the 2-dimensional scalp surface.

$$-\mathbf{E}\,(x,y) = \partial\varphi/\partial x\,\mathbf{r}_x + \partial\varphi/\partial x\,\mathbf{r}_y$$

Thus, the negative of electrical field intensity at any point, which is a vector, is the gradient of the potential there, which is a scalar. The negative sign arises from the fact that a gradient is a vector pointing in the direction of steepest ascent of the scalar field (the potential field in this case), while the force on a positive test charge is defined as positive when it reduces electrical potential (i.e., it is defined as an attractive force). Employing the 'del' operator notation, this result can be expressed as:

$$-\mathbf{E}\,(x,y) = (\mathbf{r}_x\,\partial\ /\partial x + \mathbf{r}_y\,\partial\ /\partial x)\,\varphi(x,y,z) \equiv \nabla\varphi$$

or, $$\mathbf{E}\,(x,y) = -\nabla\varphi$$

By computing at each scalp location the gradient of the EEG-recorded potential distribution φ (x,y), it is thus theoretically possible to derive the electrical field intensity distribution, E(x,y). It is then possible to derive the distribution of charge density, φ (x,y), from E(x,y), by exploiting Gauss's law and the 'divergence theorem'.

By Gauss's law the integral of the outward-oriented normal component of an electrical field over a surface surrounding a charge is equal to 4π times the magnitude of the charge:

$$\iint_S \mathbf{E}\cdot\mathbf{n}\,ds = 4\pi Q = 4\pi \iiint_v \rho\,dv.$$

By the divergence theorem, meanwhile, the surface integral of the normal component of a vector field (such as the left-hand term above) is equal to the volume integral of the 'divergence' of the same vector field, over the enclosed volume. 'Divergence' is the 'del' or gradient operator applied to a vector, and the result (their 'dot product') is a scalar. Thus,

$$\iint_S \mathbf{E}\cdot\mathbf{n}\,ds = \iiint_v \nabla\cdot\mathbf{E}\,dv.$$

The benefit of these two results is that the right-hand terms in both equations above are equal to the same thing, hence equal to each other, and they both are volume integrals:

$$\iiint_v \nabla\cdot\mathbf{E}\,dv = 4\pi \iiint_v \rho\,dv.$$

Since Gauss's law holds for any arbitrary volume, it may be assumed that if these two volume integrals are equal to each other, then their integrands are equal:

$$\nabla\cdot\mathbf{E} = 4\pi\rho.$$

But it was shown above that $E = -\nabla\varphi$, so by substitution,

$$\nabla\cdot(-\nabla\varphi) = 4\pi\rho.$$

Thus, it is possible to derive, for each scalp location, the value of the scalar quantity, charge density, by finding the divergence of the gradient of the EEG-recorded potential field at that point. The combined operation, 'div-grad' is represented by the 'del-squared' notation, ∇^2. This is the operation of taking second partial spatial derivatives (of, in this case, the voltage distribution). With this notation, the conclusion reached above may be summarized as:

$$-\nabla^2\varphi = 4\pi\rho.$$

Expanded to show the details, this is:

$$-(\partial^2\varphi/\partial x^2 + \partial^2\varphi/\partial y^2) = 4\pi\rho.$$

This operator ∇^2 is called the Laplacian, and the resulting equation for charge density is called 'Poisson's equation'. (The 'Laplacian operator' should not be confused with the Laplace transform, and Poisson's equation should not be confused with Laplace's equation, which is Poisson's equation for the special case where ρ = 0.)

To eliminate the factor 4π it is convenient to switch back to the MKSA system:

$$-\nabla^2\varphi = \rho/\varepsilon$$

or,

$$-\varepsilon\nabla^2\varphi = \rho.$$

Poisson's equation for charge density may now be exploited to obtain an equation for the energy density of the scalp electrostatic field. It is important at this point to recall that electrical potential (e.g., the potential difference measured by EEG) is the potential energy of the field (at the point where it is being sampled) per unit of charge. Thus a 'volt' is defined as one joule of potential energy per coulomb of charge. Correspondingly, one joule of potential energy is the product of one volt of electrical potential difference acting on one coulomb of charge.

Assuming that the potential energy of the scalp electrostatic field is, like charge, a 'smeared' continuum, then the potential energy at any infinitesimal point is the product of charge density and the EEG-measured potential at that point. Using the symbol 'U' to stand for this limit ratio of potential energy per unit of surface area,

$$U(x,y) = \varphi\rho$$

Substituting Poisson's equation for charge density, this becomes:

$$U = -\varepsilon\,\varphi\nabla^2\varphi.$$

This is the key result. Scalp electrical energy density can be calculated directly from the EEG voltage data, weighted by charge density information that is derived from the same data from the spatial juxtaposition of the voltage readings and therefore from the geometrical shape of the voltage field. (The value of the permittivity coefficient can be set equal to unity; it functions as a scale coefficient in displays of energy density and can be eliminated through normalization in comparative analyses.)

There is a practical issue that must be addressed, however. In EEG data, voltage is often negative. That is, the voltage level of the arbitrary body reference may be higher than the voltage level of

the scalp electrode. The Laplacian may also be of either sign, depending upon the spatial rate of change of the gradient of the scalp voltage field in the X and Y directions at the electrode site. Simply multiplying the (negative of) the Laplacian by voltage will therefore produce a confusing result. To avoid this, it is necessary to "dc-shift" the voltage data by a large enough factor to keep all voltage readings positive. To assure comparability the shift should, of course, be the same for all instants in an EEG (or ERP) time series and across all subjects and conditions in an experiment. No information is lost by this expedient. The shape of the scalp voltage surface is unaffected, but since voltage will then always be positive, the sign of the energy density calculation will always follow the sign of Poisson's equation (the negative of the Laplacian.) This is important information to preserve, since a scalp region of negative charge density would correspond to a current sink and a region of positive charge density would correspond to a current source. There may be interest in relating these to the dipoles or generator mechanisms thought to produce the scalp electrical field.

Estimation of the Voltage Surface by Regression Analysis

The mathematical derivations presented in the previous section may seem formidable. But in practice, it is only necessary to perform the following steps at each instant in the EEG record: 1.) Use the x-y grid of simultaneous voltage values to estimate the spatial distribution of voltage for that instant, 2.) calculate, for any point in question, the second-partial spatial derivatives (the Laplacian) of the estimated voltage 'surface', and 3.) multiply the result by the voltage level at the point in question.

The first step may be accomplished by multiple regression analysis. A different interpolation scheme such as cubic splines might be adequate if the only objective were to produce a 3-dimensional visualization of the scalp voltage surface. Here, however, the objective is to be able to compute the spatial derivatives of the voltage distribution, and this very easily done if one has a single equation relating voltage to scalp location. Multiple regression analysis provides such an equation. The simplest approach is to picture the scalp electrode grid as a flattened X-Y grid with voltage values plotted as distances on an orthogonal Z-axis (Figure 1).

The electrode designations shown above conform roughly to the International 10-20 system of electrode placement. Researchers may wish to experiment with a more precise grid (and even with spherical coordinates!). But the evenly spaced system shown in the figure vastly simplifies the regression analysis. Note that center of the grid is location (0,0) and the o2 occipital electrode has coordinate values X =1, Y= - 2

For each sample of electrode microvolt readings (i.e., at each instant in the multielectrode record), the objective is to find an equation that will describe the shape of the whole scalp electrode potential field. Least-squares regression analysis does that by finding for a pre-specified form of the equation, a 'model' equation -- the coefficients that make it best 'fit' the data in the sense of minimizing the sum of the squared errors. The following model equation allows for the possibility of multiple peaks and valleys in the voltage surface and also is convenient for the regression procedure:

$$Z = (a + b X + cY + eXY)3.$$

Although the equation is non-linear in X and Y, all of the X-Y combinations will have fixed values the same fixed values for all applications of the regression analysis using the same electrode placement scheme. When expanded, the equation leads to a linear polynomial in 16 terms for each electrode location. This is called the 'reduced form' of the model:

$$Z_j = [\, a3 + 3a2bX + 3ab2X2 + b3X3 + 3a2cY + (3a2e + 6abc) XY + (3b2c+6abe) X2Y + 3b2eX3Y + 3ac2Y2 + (3bc2 + 6ace) XY2 + (3ae2 + 6cbe) X2Y2 + 3be2 X3Y2 + c3Y3 + 3\ C2eXY3 + 3ce2\ X2Y3 + e3X3Y3]_j.$$

Since all of the X and Y values (and all of their powers and products) are constants, being merely the grid coordinates of the j-th electrode, this whole long equation can be reduced to: $Z_j = [=[\Sigma\ \beta_k\ Q_k]_j$

where the j-index runs from 1 to n (the number of electrodes) while the k-index runs from 1 to 16, the number of terms in the polynomial.

The Q values are the products and powers of X and Y. One may picture Q as a vector of 16 constants, and it can be precalculated for each electrode location. For example, for the occipital o2 electrode, with grid coordinates X=1, Y= -2, the Q-vector is:

(1, 1, 1, 1, -2, -2, -2, -2, 4, 4, 4, 4, -8, -8, -8, -8)

Meanwhile, the β values are the various combinations of the coefficients, a, b, c, and e in the expanded equation. For instance, $\beta_1 = a^3$ and $\beta_2 = 3a^2b$. Without knowing their values, one may picture the β values as a vector too. Therefore, in matrix notion the reduced form is simply:

$$Z_j = \beta^T\ Q_j$$

(1x16) (16 x 1)

where the superscript-T indicates that the β-vector is transposed. It is not necessary (or possible) to "identify" the coefficients, a, b, c, and e in the underlying model equation. The energy density estimate will depend strictly upon the estimated values of the β coefficients.

The β-vector is the set of 16 coefficients to be estimated. Since the whole objective of the least-squres procedure is to find a single set of these coefficients that will give the model surface the best fit to the observed voltage values at all of the electrodes, the β-vector will be the same vector for each electrode postion (each Zj equation shown above). This means that one may introduce a matrix, R, each row of which is a Q-vector (transposed) like that shown for the o2 electrode above.

This allows the reduced form equations of the model for all (n) electrodes together to be expressed as:

$$Z = R\ \beta$$

(n x 1) (n x 16)(16 x 1)

If the β-vector had already been estimated, the actual electrode voltage observations could be compared to the estimate to obtain a

measure of the error or deviation, uj for the j-th electrode:

$$u_j = Z_{actual}\,(X, Y)_j - Z_{est}\,(X,Y)_j$$

Correspondingly, for the whole set of electrodes, this comparison produces a u-vector:

$$u = Z_{actual} - R\,\beta_{est}$$

$$(n \times 1)\ (n \times 1)\ \ (n \times 16)(16 \times 1)$$

The object of 'least squares' regression analysis is to find the β values that will minimize the sum of the squared errors. This is a straight-forward application of matrix calculus. The first step is to expand the matrix expression for the sum of the squares:

$$\mathbf{\Sigma}\, u_j^{\,2} = u^T u.$$

$$= (Z - R\,\boldsymbol{\beta}_{est})^T (Z - R\,\boldsymbol{\beta}_{est})$$

$$= (Z^T - \boldsymbol{\beta}_{est}^{\,T} R^T)\,(Z - R\,\boldsymbol{\beta}_{est})$$

$$= Z^T Z - 2\,Z^T R\,\boldsymbol{\beta}_{est} + \boldsymbol{\beta}_{est}^{\,T} R^T R\,\boldsymbol{\beta}_{est}$$

These manipulations take advantage of two facts. First, in general, for any two conformable matrices A and B it can be proved that $(A\,B)^T = B^T A^T$ Secondly, the term $Z\,T\,R\,\boldsymbol{\beta}_{est}$ is (1 x 1), a scalar, and hence equal to its own transpose. Thus, it appears twice.

Now the calculus step: In order to minimize the final equation (for $u^T u$) its first derivative with respect to $\boldsymbol{\beta}_{est}$ is set equal to zero and the resulting equation is solved for the value of $\boldsymbol{\beta}_{est}$:

$$0 = \boldsymbol{\partial}\, u^T u\ /\ \boldsymbol{\partial}\,\boldsymbol{\beta}_{est}$$

$$= \boldsymbol{\partial}\,(Z^T Z - 2\,Z^T R\,\boldsymbol{\beta}_{est} + \boldsymbol{\beta}_{est}^{\,T} R^T R\,\boldsymbol{\beta}_{est})\ /\ \boldsymbol{\partial}\,\boldsymbol{\beta}_{est}$$

$$= -\,2\,R^T Z + 2\,R^T R\,\boldsymbol{\beta}_{est}$$

Hence $\boldsymbol{\beta}_{est} = (R^T R)^T (R^T Z)$

Recall that every element of R is a constant (the rows of R are the Q-vectors for each electrode). This matrix can therefore be computed once, in advance, to be used in all applications employing the same electrode placement pattern. The same is true for a new matrix, A:

$$A = (R^T R)^T R^T$$

$$(16 \times n)\ (16 \times 16)\ (16 \times n)$$

Thus, $\boldsymbol{\beta}_{est} = A\,Z.$

$$(16 \times 1)\ (16 \times n)\ (n \times 1)$$

There will be a Z-vector (a set of electrode voltage values) for each sampling instant in the EEG record. For each instant in the record a new set of **β** coefficients must be estimated. But this can be achieved quickly by simple pre-multiplication of the Z vector by the same A matrix.

To plot the estimated voltage field at any instant as a smooth surface it is only necessary to compute a Q-vector for each (arbitrary) grid location and pre-multiply it by the transpose of the estimated **β**-vector for that sampling instant.

It also is possible to compute the first and second partial spatial derivatives at any (arbitrary) grid location. This is most easily accomplished by first deriving these derivatives for the algebraic expression for the reduced form of the equation for Z, expanded in the 16 products and powers of X and Y. For instance, the first partial derivative with respect to X will be:

$$\partial\, Z\ /\ \partial\, X = \beta_2 + 2\beta_3 X + 3\beta_4 X^2 + \beta_6 Y + 2\beta_7 XY + 3\beta_8 X^2 Y + \beta_{10} Y^2 + 2\beta_{11} XY^2 + 3\beta_{12} X^2 Y^2 + \beta_{14} Y^3 + 2\beta_{15} XY^3 + 3\beta_{16} X^2 Y^3.$$

The β-coefficients having been estimated for the particular instant in the EEG record, it is then a simple matter to substitute the X and Y values for the grid location of interest. For instance, for the o2 location, X = 1, Y = -2:

$$\partial\, Z\ /\ \partial\, X = \beta_2 + 2\beta_3 + 3\beta_4 - 2\beta_6 - 4\beta_7 - 6\beta_8 + 4\beta_{10} + 8\beta_{11} + 12\beta_{12} - 8\beta_{14}^{\,3} - 16\beta_{15} - 24\beta_{16}$$

Although the regression procedure seems complex when all of the derivations are spelled out, it actually is a remarkably simple when it is applied. All that is necessary is to perform the following steps: 1.) Pre-compute the A matrix, which is determined completely by the grid coordinates of the electrodes. 2.) At each instant in the multielectrode record estimate the β-coefficients by post-multiplying A by the vector of voltage readings. 3.) To display the voltage surface, estimate the height of the surface at each location of interest by computing a Q vector for that grid location and remultiplying it by β. 4.) To compute the second partial spatial derivatives for the Laplacian, substitute the grid locations for each electrode site into expressions for the derivative like that shown above. 5.) To estimate charge density at the electrode locations, simply add the second partials and reverse the sign of their sum. 6.) To estimate energy density, multiply the charge density estimate by the voltage for the corresponding position.

One might ask, how good is the regression fit, upon which the rest of the procedure depends? In order to assess the quality of the fit, the time series of estimated values of voltage for various electrode sites has been compared with the original EEG data. For any given instant in the data, the R-square value, was always very high, for example around 0.97, and consequently the time series for the estimated voltage data almost exactly matched the actual data.

It is reasonable to assume that the quality of the regression fit depends upon the number of electrodes in the grid. However, this is a more complex issue than might be expected. First of all, it is essential that the number of electrodes exceed the size of the $(R^T R)^T$ matrix, which is 16 x 16 for the model equation $Z = (a + b\,X + cY + eXY)^3$. The R-square value cited above was based on 21 electrodes (those shown in the grid diagram presented earlier).

An experiment was conducted to see the effect of using a grid of 36 electrodes. The fit deteriorated remarkably. From one instant to the next in time series the R-square value for the spatial fit fluctuated wildly. Hence the estimated time series poorly represented the actual data. With so many electrodes, the spatial correlation among them produced severe 'multicolllinarity'. [7] (Kementa, 1971).

The Gauss-Markov theorem assures us that least-squares regression produces the "best linear unbiased estimate" of the b-coefficients. But this requires several assumptions about the data, such as independence among the exogenous variables. (cf. Johnston, 1963). Research data never perfectly conforms to these assumptions; and some degree of multicollinearity is always present in applications of multiple regression analysis. The practical issue

is how serious it is. Apparently, the problem is far less serious for 21 electrodes than for 36. There may be an optimal number of electrodes (24?), but this issue was not explored since the 'standard' pattern of 21 did the job so well.

On the other hand, there is an important implication of the finding that multicollinearity became a serious problem with just 36 electrodes. There is currently much interest in creating very dense electrode grids in the expectation that this will improve the spatial resolution of EEG. The finding mentioned here indicates, however, that the scalp electrostatic field, at any instant, is spatially characterized by gentle gradients, even though EEG time series may contain abrupt oscillations (for conventional chart strip recording speeds). Adding electrodes apparently did not reveal independent peaks and valleys.

Computer Implementation

The flowsheet shown below summarizes the procedure, which is assumed to start with an ERP (i.e., an average of, say, sixty artifact-free, stimulus-gated multielectrode EEG epochs). The following describes the computer implementation of the procedure:

Creation of an A-Matrix

Recall that the regression coefficients for each successive voltage surface in an ERP are obtained by pre-multiplying the vector of electrode site voltage readings by single matrix:

$$A = (R^T R)^T R^T$$

$$(16 \times n) \quad (16 \times 16)(16 \times n)$$

This A-matrix should be computed in advance and stored as a library file. The computation requires no input data, but it does obviously require the R-matrix, which can be computed at the same time. Each row of the R-matrix is a Q-vector, (i.e., the sixteen combinations of products and powers of X and Y) numerically resolved for each of the n-electrode positions.

Data editing

Computation of the R-matrix establishes a fixed sequence for the electrode positions. Therefore, it probably will be necessary to reformat the ASCII files exported by various EEG systems. This editing step might be done by a separate program to perform this and other housekeeping tasks:

- Moving the input data into a standard output format, which, viewed as a matrix, presents each time sample (instant in the ERP) as a row, with a column for each electrode site.
- Reshuffling the order of the electrode data to fit a standard ordering of the columns (as required by the R-matrix). Also, in many standard montages, the lead for the center occipital electrode, oZ, has been used for recording other data, or is missing. At this point it is useful to recreate this electrode's data as an average of o1 and o2 (Figure 2).
- Skipping initial time samples in the raw data, if necessary. This depends upon whether the imported ERP allows for a time period prior to the stimulus, and whether that is to be allowed for in subsequent analyses.
- Smoothing the input data, for example, by a moving-average filter. Some degree of smoothing is usually desirable, since sharp peaks and other discontinuities in the original ERP will create havoc in the computation of the derivatives.

Importing Files and Adjusting the Edited ERP Data

Steps 1 and 2 are best performed by separate programs. From here on, the steps are assumed to be subroutines of the energy-density estimation program itself. The first subroutine would naturally import the file representing the A-matrix and the edited ERP file. The latter file requires two adjustment steps:

- First, assuming that the electrode assignment for the R matrix was for a regular square grid (e.g., 5 x 5), it may be necessary to create pseudo-electrode data for the corner positions, which are absent in most EEG montages. Several experiments indicate that this is best done by simply averaging the three electrode values adjacent to the missing corner.
- Second, a fixed constant, greater than any negative excursion in the ERP data, should be added to every input data value. This amounts to a dc-shift of the ERP data, sufficient to keep all the voltage readings positive. (It also is equivalent to moving the body reference electrode to a position such that it will always have a voltage value lower than that of any electrode.)

Although these two adjustments to the ERP input file could have been performed in the editing program, performing them here preserves the edited (and smoothed) ERP in a form that is similar to the original ERP. The edited ERP data will still have the same number of electrode (no corner positions) and it will still have the negative excursions.

Regression estimation of voltage surface

Assuming a 5 x 5 grid, the result of the previous step is a vector of 25 electrode values for each instant in the ERP. This is the Z-vector. The regression coefficients for the estimated voltage surface can now be quickly computed by pre-multiplying the A matrix by this vector:

$$\beta_{est} = A Z.$$

$$(16 \times 1) \; (16 \times n)(n \times 1)$$

Computation of derivatives for the Laplacian

Immediately, the first and second partial derivatives can be computed, in the X and Y directions for each electrode position. Recall that these derivatives involve products and powers of X and Y, multiplied by some of the β-values. It is best to represent these derivatives as algebraic polynomials in the program, and then to iteratively substitute the appropriate values for X and Y for each electrode site along with the current estimated β-values.

Computation of charge and energy density

Still operating on a given time sample (row in the edited ERP file), the values of the charge and energy density estimates for that instant can now be computed for each electrode site.

$$\text{Charge } (X,Y) = -(\partial^2 \varphi / \partial X^2 + \partial^2 \varphi / \partial Y^2)$$

$$\text{Energy } (X,Y) = \varphi (X,Y) \times \text{Charge } (X,Y)$$

Here, φ (X,Y) is the estimated voltage surface, and constants such as permittivity are implicitly set equal to unity. These charge and energy density estimates should be stored (in the appropriate columns) as rows in two matrices that can eventually be exported as charge and energy density versions of the ERP.

Iteration for Each Time Sample

At this point, the program should loop back to step 4 until the last row of the (edited) ERP is finished. If it is finished, then the charge and energy density ERPs can be exported as files for subsequent analyses and displays. Since different experiments may involve different sampling rates it is useful to include this information in the file designations, so that it may automatically adjust the time axis in various display programs. Also, it may be necessary to adjust the scale of the energy and charge density data to make these time series visually comparable to each other and to the voltage data.

Depending upon the researcher's intentions, it may be useful to incorporate display routines within this program itself. Since the β-values are available (after step 4) these may be used immediately to compute the estimated voltage values at a sufficient number of grid locations to create a smooth picture of the estimated voltage surface. Similarly, by substituting a sufficient number of grid locations (X and Y values) into the Laplacian, smooth surfaces can be displayed for the charge and energy-density surfaces. Given the speed of modern desktop computers this will likely be quicker and more convenient than pulling the saved charge and energy density ERPs into a separate graphics program.

The computer code reproduced in Appendix A accomplishes steps 3 through 7 in Turbo-Basic. Note that, at line 232, the A-matrix had been given the file name CXPXI and was labeled XXX in the program. Also note that the program was designed to output either a charge-density ERP or an energy density ERP, depending on the value given to the variable DS at line 12. This arrangement could easily be changed, so that both ERPs are automatically exported. Finally, note that a graphic display routine could be included after line 700, in which case the variable ST at line 705 should be reduced to, say, 0.1, in order to compute enough points for a smooth surface. If-Statements should then be added to line 706 to prevent calling SUB 2000 except when W and V are both integers with values 1, 2, 3, 4, or 5.

Derivation of Electroencephalographic Energy-Density

We have been able to precisely quantify the relationship between subjects' performance on a standardized cognitive task and their level of cortical activation at selected EEG electrode sites at particular times. Detailed discussions of this and related work can be found in Montgomery and Gleason [8]; Montgomery, Montgomery and Guisado [4,8] and Montgomery and Guisado [5].

The key step facilitating this success is the mathematical transformation of conventional voltage event-related potentials (ERPs) into temporal and spatial profiles of the underlying scalp distribution of energy-density as described in Sections II and III. Others [3,9,10] have noted that relatively brief and localized cortical electrical events may initiate complicated spatial-wave patterns of disturbances in the scalp electrical field. Hence, the spatial contours of the field may be more important than the separate time profiles recorded at individual electrode sites.

We agree that it is essential to look at the evolving shape of the whole scalp electrical field following a cognitive stimulus. In addition, we have found that it is important to look at the scalp distributions of charge- and energy-density as well as voltage.

Conventional ERPs are constructed by time-averaging an ensemble of stimulus-gated voltage recordings at an electrode site. Aside from any ambiguity that arises from the fact that voltage can only be measured relative to an arbitrary "reference electrode", voltage has another inherent ambiguity: voltage is a measure of potential energy per unit charge. Therefore, unless the charge concentration at the point in question is also known, the electrical energy of the field cannot be approximated. Our approach overcomes this ambiguity and converts conventional ERPs into energy-density profiles that can be used in the regression of performance upon cortical energy-density. The approach can be explained most easily in terms of the successive substitutions in the following equations, where all empirical and scale constants have been arbitrarily set equal to unity:

$$\text{Energy Density} = \frac{\text{Potential Energy}}{\text{Area}}$$

$$= \frac{\text{Potential Energy}}{\text{Charge}} \times \frac{\text{Charge}}{\text{Area}}$$

$$= \text{Voltage} \times \text{Charge Density}$$

$$= \text{Voltage} \times (-1) \times \text{Laplacian of Voltage}$$

$$= V \cdot \nabla^2 V$$

The "Laplacian" of voltage (at any scalp location) is the sum of the second partial spatial derivatives of voltage with respect to the two orthogonal surface directions (the spatial coordinates of the electrode grid).

$$\nabla^2 V = \frac{\partial^2 V}{\partial x^2} + \frac{\partial^2 V}{\partial y^2}$$

In a geometrical sense it is simply a number which indicates the relative curvature of the voltage surface. In 1842 William Thompson (Lord Kelvin) recognized that this number would be proportional to the spatial distribution of electrical charge (the negative sign reflects the definition of electrical force as positive when it is repulsive). Thompson also recognized that it is possible to multiply the Laplacian by voltage to obtain energy-density [11,12]. Thompson's insight was later formalized by Maxwell [1,6,13-15].

The Laplacian (the second spatial derivative operator) should not be confused with the "Laplace transform", which is an entirely different mathematical concept, used to study the frequency-domain response functions of dynamic systems.

We believe we are the first to apply this approach to EEG data. The Laplacian by itself has been recommended as a means of revealing the locations of sources of polarization currents from the cortex, through the skull, onto the scalp. [2,3,16,17] However our procedure involves an additional step: the multiplication of the Laplacian by voltage at each location.

The usual approach to estimation of the Laplacian of the scalp electrical field at each instant is by spatial interpolation from the voltage levels recorded at the individual electrode sites. We have found, however, that better results are obtained by least-squares estimation of the contours of the voltage surface, followed by vector calculus transformation of the fitted surface into its Laplacian. The least-squares estimates of the voltage surface provide the necessary estimate of the values of voltage between electrodes; and the fitted model equation conveniently facilitates taking the second partial spatial derivatives, which are required for the Laplacian.

Using X and Y to represent grid locations, the model equation is:

$$\text{Voltage at grid location } X_i, Y_i = (a + bX_i + cY_i + dX_iY_i)^3$$

Expanded, this becomes

$$\text{Voltage}(X_i, Y_i) = \left(b_1 + b_2X_i + b_3X_i^2 + \ldots + b_{15}X_i^3Y_i^2 + b_{16}X_i^3Y_i^3\right)$$

In this equation there are sixteen coefficients to be determined by the least-squares algorithm. The algorithm finds that set of coefficients that minimizes the sum of the squared values of the "errors", i.e., the differences between actual and estimated voltage over all electrode positions.

At a sampling rate of 128 Hz, this approach implies 128 least-squares estimates for each second's worth of data. However, the procedure is very rapid due to the fact that the set of X and Y values (the independent variables) is fixed, being the fixed electrode locations. This set of fixed values corresponds to the "design matrix" of a general linear model and the time-consuming matrix inversion step required for least squares needs to be performed only once for a given electrode configuration.

We have found that a grid of 21 electrodes produces an exceptionally good estimate of the voltage surface. When voltage values derived from the fitted surface are compared with the raw data at the electrode sites, the value of R-square is typically 0.92 or better. Figure 1 shows the estimated voltage compared with the actual voltage data for a typical EEG montage. (Only 18 of the 21 electrodes are shown in order to keep the figure from being too crowded) (Figure 3,4).

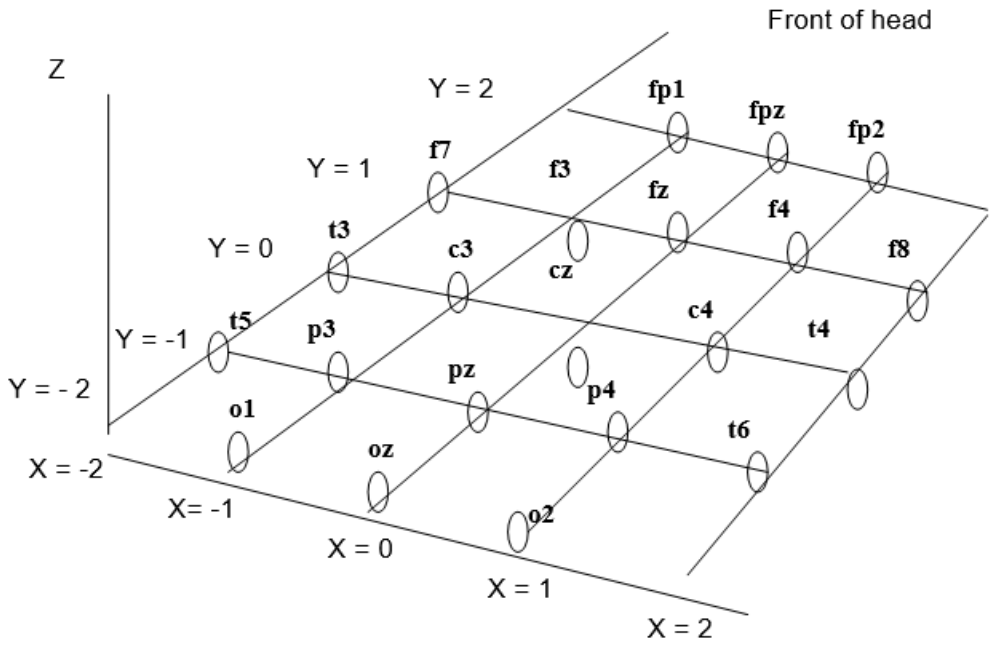

Figure 1:

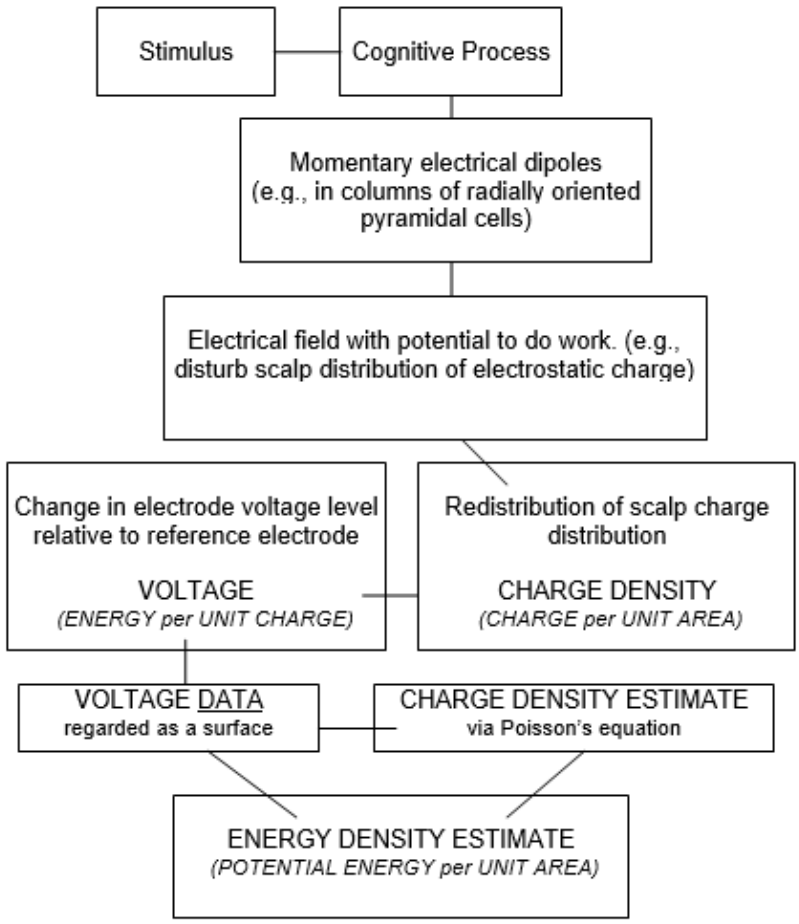

Figure 2: Flow diagram for estimation of energy-density ERPs

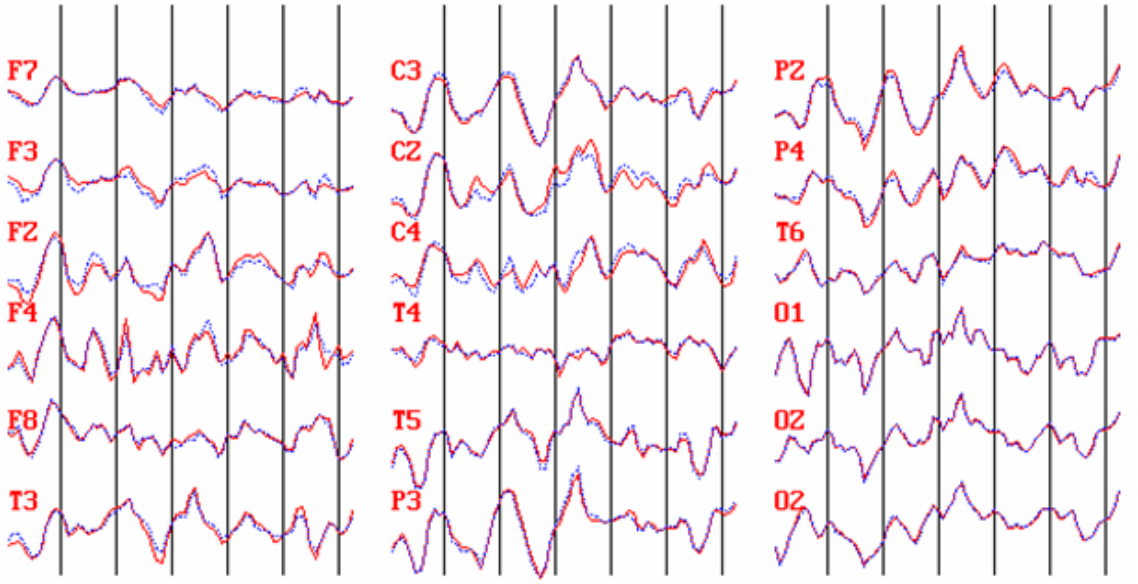

Figure 3: Comparison of raw EEG data (solid line) and estimated (dotted line) values using fitted regression model.

For reference, Figure 3 shows the electrode locations; this is the International Standard "10-20" system of electrode assignment.

The following is an example of a multielectrode recording from a grid such as that in Figure 3 (Figure 5).

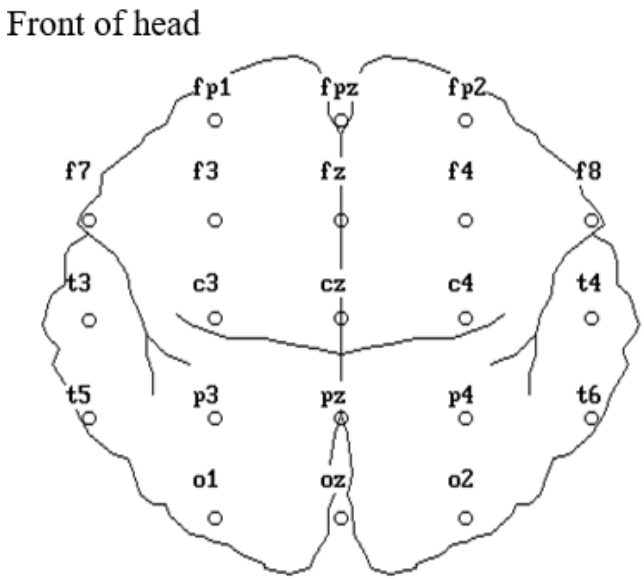

Figure 4: Electrode locations for the International '10-20' system.

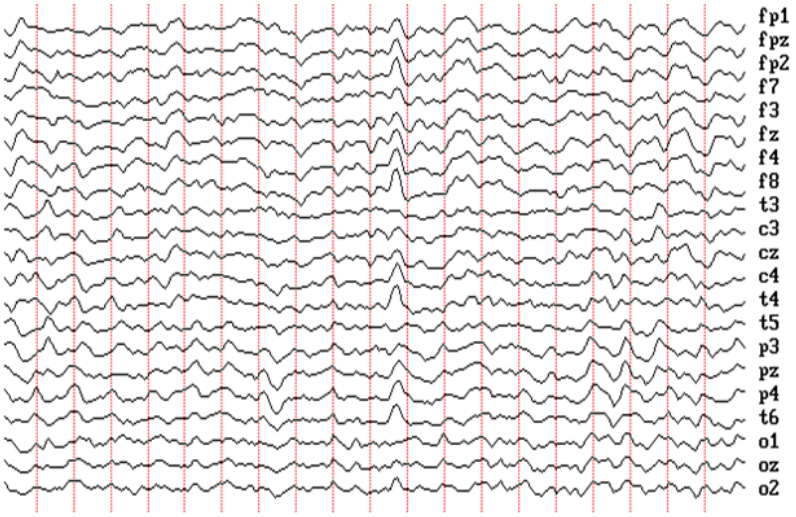

Figure 5: Two-second multielectrode EEG voltage recording Vertical lines mark 100 millisecond intervals.

It is possible to view the set of voltage readings -- at any instant -- as a sample of points describing a voltage surface, as illustrated in Figures 6 and 7 (Figure 6).

If the grid contains a sufficient number of electrodes, interpolation methods, such as least-squares, may be used to fill in the blanks. The following figure illustrates the result, based on the data in Figure 6 (Figure 7).

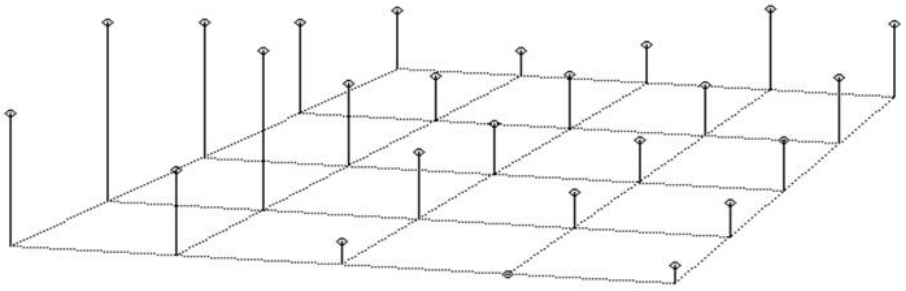

Figure 6: Voltages at each electrode at one instant in the recording. Positive voltage plotted upward; grid oriented with the front of the subject's head to the viewer's right.

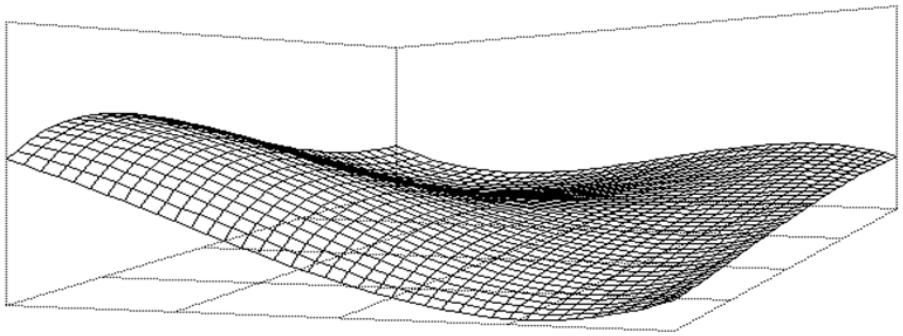

Figure 7: Least-squares surface fitted to the voltage data shown in the previous figure. Positive voltage upward, electrode grid oriented with the front of the subject's head to the viewer's right.

Application of the Laplacian to every point (every x, y value) in the estimated voltage surface shown in Figure 7 produces the following estimate of charge-density (Figure 8).

Having calculated the surface charge-density distribution corresponding to an instant in the multielectrode EEG data, surface charge-density multiplied by voltage leads to surface energy-density. In the MKS system the units are Joules per square meter (Figure 9).

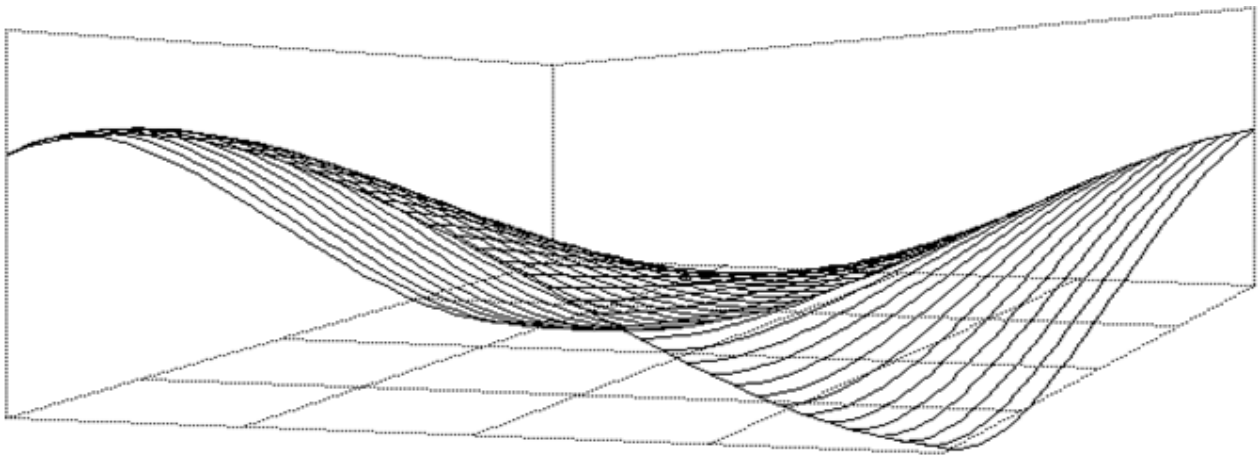

Figure 8: Charge-density surface corresponding to Figure 7.

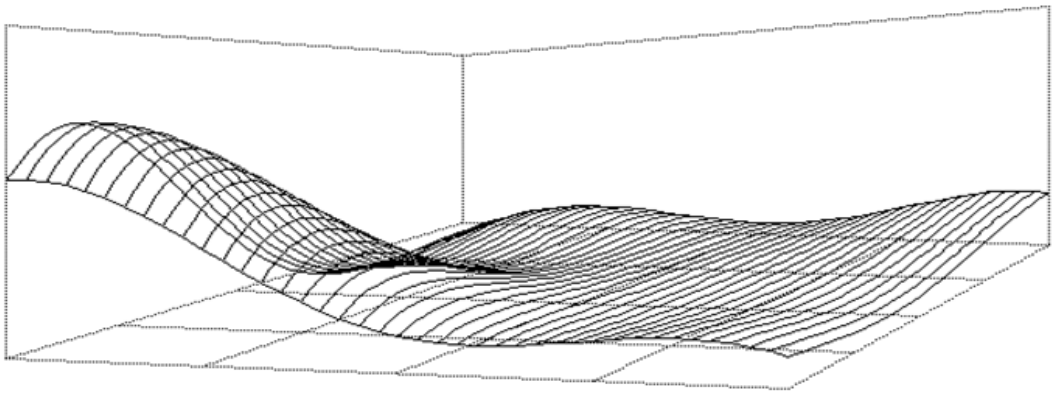

Figure 9: Scalp surface potential energy distribution derived from Figures 7 and 8.

The energy-density mathematical transformation of topographic electroencephalographic data is then used to identify locations of neural activity that are directly related to task performance. A regression analysis is conducted across all subjects, at each sampling period during the subjects' ERPs and at each electrode site, to correlate the groups' task performance and neural activity.

Correlations, as described above, made for each electrode site and time period during the ERP can be used to identify positions on the scalp, and times, for which the subjects' neural activity is highly correlated with task performance. These areas of high correlation, which shift from one cortical region to another over the course of the task ERP, can be identified using multiple regression techniques.

To date, all applications of EEG to experiments regarding cognition or task performance have used only the voltage data. The high correlations of neural activity on performance discussed above could not be obtained using conventional voltage ERPs. Energy-density transformations improve both the spatial and temporal resolution of measured neural activity.

The use of our energy-density procedures in cognitive research offers one more advantage over conventional EEG measures of neural activity; resultant values can be integrated over both time and location. Neural activity from specific regions as well as single electrode sites of the brain can be investigated and correlated with task performance.

Previous EEG Energy-Density Research

Although the concept of mapping scalp charge-density distributions from multi-electrode voltage data has been discussed in the EEG literature [2,3] (1989) our research applies this concept to experiments involving comparisons of cognitive ERPs. We also have developed techniques for using the deriving energy-density ERPs from the voltage data in cognitive research. This section describes four of our recent studies that lead us to believe that energy-density and or charge-density ERPs can used to predict performance deterioration during a sustained cognitive task.

Study 1: Cross Subject Comparisons of Mental Arithmetic Performance

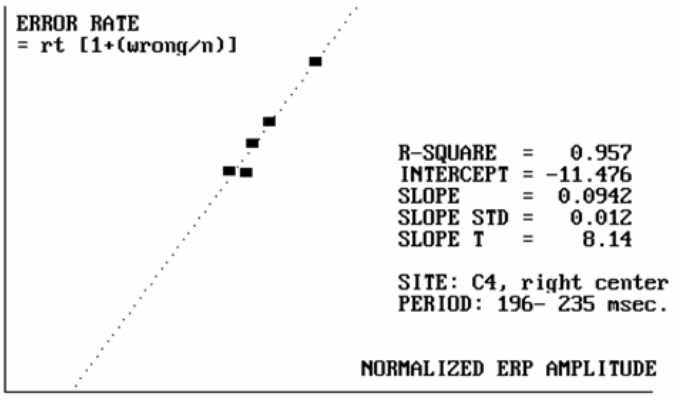

Figure 10: Regression of five subjects' mental arithmetic error indices on their scalp-surface energy-densities at right central site, C4, averaged over post-stimulus period 196-235 ms.

As part of a NASA-sponsored SBIR Phase II contract (NAS1-18847), we collected energy-density ERPs from healthy adult (right-handed male) subjects as they performed various cognitive tasks presented via a computer screen. In post-hoc analysis of the data we discovered very high correlations between subjects' relative performance and the amplitudes of their energy-density ERPs at particular electrode sites and post-stimulus latencies. Figure 10 is an example. This figure shows that a linear regression line almost perfectly describes the relationship between the subjects' error rate on the mental arithmetic task (vertical axis) and scalp-recorded energy-density (horizontal axis) (Figure 10).

One reason we are proposing to use energy-density ERPs to monitor cognitive performance is that relationships like that in Figure 8 simply do not appear in conventional voltage ERPs. Comparison of Figure 10 with Figure 11 shows the difference. Both figures come from exactly the same data, except Figure 11 uses the original voltage ERPs (Figure 11).

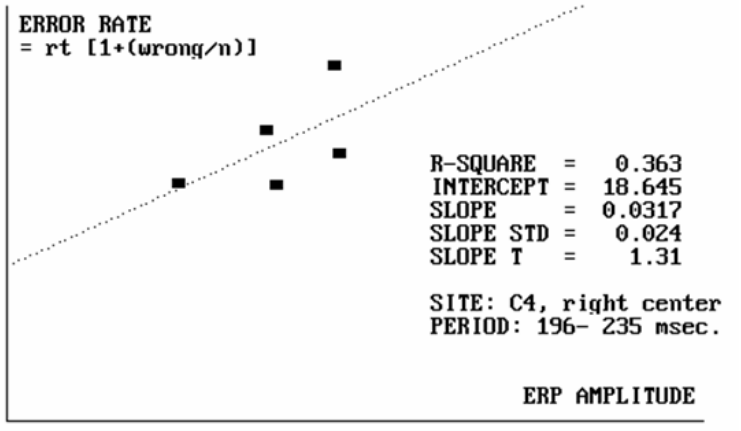

Figure 11: Regression of five subjects' mental arithmetic error indices on their (conventional voltage) ERPS at the same electrode location and time period as shown in Figure.

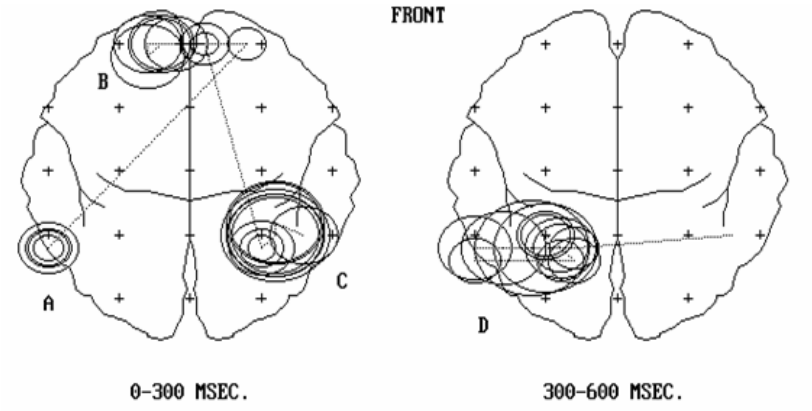

Figure 12: Locus of peak cross-subject correlations between mental arithmetic performance and scalp-surface energy-density.

When we mapped sites of similar high correlations, we found the locus or path of performance-correlated cortical activity shown in Figure 12 (Figure 12).

The diameters of the circles in the figure are proportional to the correlation coefficients at the sites at the centers of the circles. This finding is consistent with current hypotheses about the localization of cognitive function during mathematical processing. For example, studies of patients' deficits in cognitive performance following gunshot wounds or other cortical lesions have indicated the importance, for mental arithmetic, of an area near the left angular gyrus [18-21]. Our EEG research adds additional dynamic detail. There appears to be four stages in which localized cortical activity is highly correlated with mental arithmetic performance:

A. Preparatory response in the left temporal-parietal area, 89 – 94 msec.

B. Executive-planning response in the left prefrontal lobe, 118-157 msec.

C. Spatial analysis in the right parietal lobe, 180-243 msec.

D. Highest level arithmetic processing in the left parietal region, 244-391 msec.

Voltage ERPs have been used very successfully to identify sites of cortical activation that are correlated with the nature of the stimulus. However, these are not necessarily the sites where the level of activation is correlated with intersubjective differences in cognitive performance. For example, a visually presented cognitive task will produce a large voltage excursion in the occipital electrodes for all healthy subjects, but this 'mandatory' processing event may not be highly correlated with differences in their performance, simply because it is common to all subjects. On the other hand, differences in relatively smaller levels of activation at other sites may be related to differences in their capacity to perform the task. We found that the energy-density ERPs can reveal these more subtle correlations.

Study 2: Energy-Density Comparison of Dyslexic and Normal Readers

In collaboration with Dr. Alvirda Farmer (Communicative Science Department, San Jose University), we employed a similar procedure to see if it would distinguish between reading-impaired college students and age, sex, and IQ-matched normal readers.

Figure 13 is an example of our findings. As in the mental arithmetic project described above, the vertical axis in the figure shows the subjects' error-rates on the task -- except in this case the task was to identify pairs of words as either synonyms or antonyms. (Word pairs were presented randomly on a computer screen, without repetition, from a very long list, judged to be of similar difficulty.) The horizontal axis shows the subjects' corresponding energy-density at the center occipital electrode site, oZ, 200 milliseconds after stimulus presentation (Figure 13).

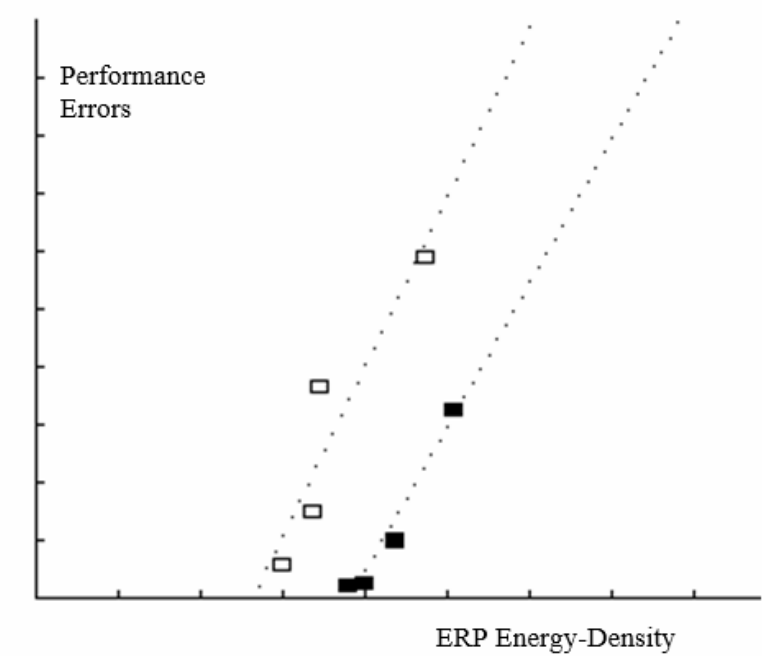

Figure 13: Semantic task performance vs. Oz energy-density, (200 msec.): Dyslexic readers (filled squares), Normal readers (open squares).

The figure shows that the energy-density ERP analysis does indeed separate the eight subjects into the two groups. It is important to notice that the subjects' error-rates, alone, would not have separated them into the two groups. Some of the dyslexics actually performed better than some of the normal readers. The separation between the two lines, shows that the procedure can reveal differences in performance capacity (correlated with the test battery results by which the dyslexics were identified) which were not evident in the immediate experimental results.

This finding is important in that it may provide a means of predicting operators' cognitive performance deterioration before it actually occurs. In order to accomplish this, it will be necessary to find a feature of the energy-density ERP that is not only correlated with performance, but which changes systematically with fatigue.

Study 3: Multiple Sclerosis Patients' Visual Evoked Responses

Although the two studies cited above depended upon energy-density ERPs, we have found that charge-density ERPs also are useful in certain applications. We participated in a project that assessed the efficacy of therapeutic cooling for cognitive performance of multiple sclerosis patients. The EEG aspect of this project involved analysis of 'visual evoked responses (VEPs)' from 18 MS patients and 17 healthy controls. VEPs are occipital ERPs for the primary visual-processing period when the stimulus is a reversing checkerboard.

VEPs are often used for clinical assessment of the integrity of the visual pathway, and the literature reports that they are often abnormally shaped for MS patients. Our project sought to determine if their VEPs become more 'normal' after a period of head and torso cooling -- and if the degree of 'improvement' in the shape of the VEP was correlated with their improvement in performance. (Cognitive performance was measured in terms of a composite of scores on the Rao [22] test battery, commonly used for diagnosing MS patients.)

At first, our finding was negative. Although the MS patients' voltage VEPs were abnormal, as the literature predicted, there was no systematic change after cooling. However, as soon as the VEPs were converted to charge-density profiles (which we call VEQs -- Q for charge), systematic post-cooling changes were observed, which were also correlated with cognitive improvement.

More importantly, we discovered that the extent to which a patient's pre-cooling VEQ differed from the normal shape could be used as a predictor of post-cooling improvement in cognitive performance. As a measure of the extent to which patients' VEQs differed from normal, we compared the integrals of their VEQs over the period 70-200 milliseconds with a similar integral for healthy control subjects' grand average VEQ. In effect, this uses the amplitude of excursions in the VEQs as simple indices of occipital cortical activation during this period, which roughly brackets the period of primary visual processing [23-30].

Figure 14 shows the relationship that we found. The vertical axis shows the patients' improvement on the Rao test. The horizontal axis shows their VEQ integral as a percentage of the normative VEQ integral. The shape of the fitted curve reveals that MS patients with nearly normal pre-cooling VEQs are not helped by cooling. The Relationship is generally inverse (except for extremely impaired patients). This finding makes sense when it is recognized that the cooling procedure may itself be distractive, and this distraction may be more important than any neural conduction benefit for patients whose visual pathway is only slightly impaired (Figure 14).

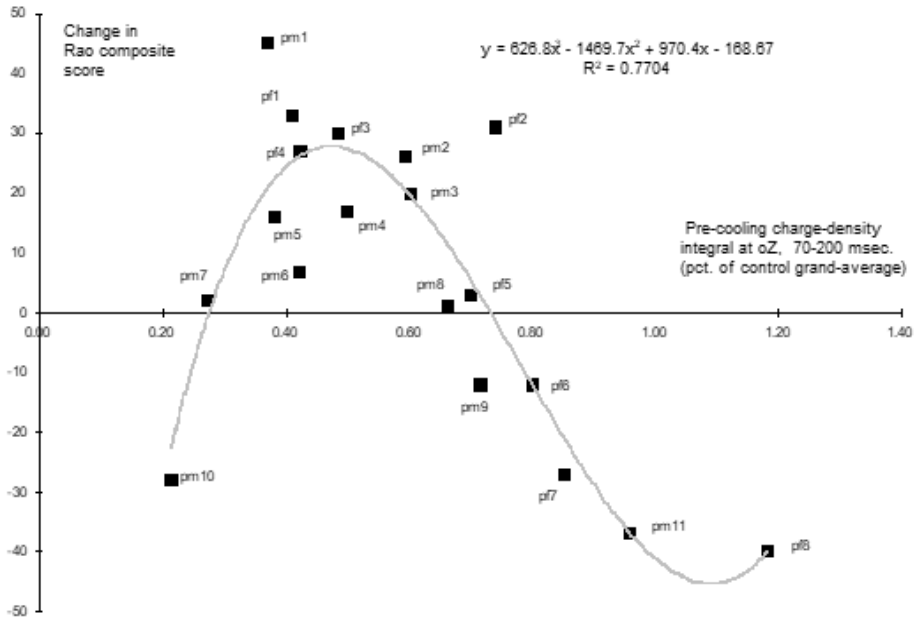

Figure 14: MS patients' post-cooling Rao Score change vs. the 'normality' of their pre-cooling charge-density VEP.

The relevance of this project is that it demonstrates the value of comparing individual ERPs with a normative ERP. Our approach to predicting operators' performance deterioration during a prolonged task is to collect an ERP early in the task, and then keep comparing it with ERPs taken periodically during the task. Ideally, we would find that the subsequent ERPs become progressively 'abnormal.'

Study 4: Monitoring Cognitive Fatigue in A Mental Arithmetic Task

One of our most recent projects used the, above mentioned, approach (comparison of successive ERPs) to assess mental fatigue. Six men and six women were asked to perform a mental arithmetic task repeatedly for up to three hours. The task consisted of indicating, by pressing a computer key, whether the sum of two random four-digit numbers was equal to, less than, or greater than a target number that was randomly generated from the set of five numbers bracketing the correct answer. The problems were presented on the computer screen; each one was presented one-half second following the subject's decision with respect to the previous one.

ERPs were produced from the first 60 to 100 artifact-free, stimulus-gated EEG epochs recorded during each 15-minute period. Subjects who lasted three hours thus produced a sequence of 12 conventional voltage ERPs which were then converted to energy-density ERPs.

We found that it was very useful to monitor, in these ERPs, the average energy-density at electrode site p3, over the post stimulus period 100-300 msec. This value appears to evolve in a systematic manner over the period of the subject's endurance, and there is a systematic relationship with the subject's error index. Figure 15 is a typical subject's response during a prolonged mental arithmetic task [31-38] (Figure 15).

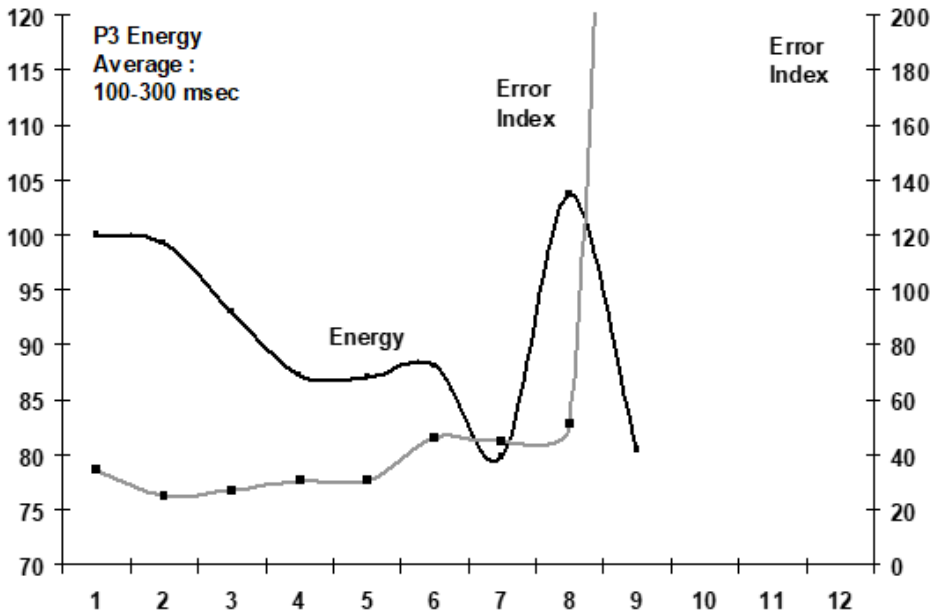

Figure 15: Typical subject's energy-density at electrode P3 and error index vs. time (each increment is 15 minutes long).

At first, the subject's energy density at p3 seems to be higher than necessary. For, over the following forty-five minutes, the energy at that site (presumed to be an arithmetic processing center) falls, without severely impairing performance. We interpret this to be a redeployment of metabolic resources to other cortical centers to support other concurrent tasks, such as homeostasis maintenance. However, the subject apparently becomes aware of the slight performance deterioration associated with this redeployment, and the energy level of p3 stabilizes or even increases slightly. But then, as soon as performance stabilizes, the redeployment begins again. Indeed, after the first hour or hour-and-a-half the energy level at p3 begins to drop precipitously. We interpret this as evidence that other, neglected brain activities are beginning to make urgent demands upon metabolic resources. This phase is highly predictive of collapse of performance -- even though the subject, evidently sensing that fact, makes an apparently desperate effort to re-concentrate cortical resources at p3. This is the spike in energy which, in Figure 14, starts at the 7th ERP (1 hr, 45 min.). By the 8th ERP (2 hours) the subject has essentially given up [39-45].

Our interpretation of this sequence of events is highly conjectural, of course. Nonetheless, the figure is quite typical, and we feel that it is significant that:

1. Energy almost always falls, and in a stair-step fashion, until the final burst.
2. Performance is not severely affected until the last step-down, which is predictive of sudden deterioration about one-half hour later.

Conclusion

Cortical energy density mapping in this manner appears to be a valuable means of tracking cortical activation during the performance of cognitive tasks under various experimental conditions. By transforming EEG data (particularly ERPs) to show energy-density distributions, EEG can be used in a similar manner. EEG is a far simpler procedure, and one that allows much more flexibility in experimental design. The use of our energy-density procedures in cognitive research offers one more advantage over conventional EEG measures of neural activity; resultant values can be integrated over both time and location. Neural activity from specific regions as well as single electrode sites of the brain can be investigated and correlated with task performance .

Acknowledgement

This work was supported, in part, by NASA-Langley Research Center, Small Business Innovative Research Phase II Contract No. NAS1-18847. The authors wish to acknowledge and thank Drs. Alan T. Pope and Raul Guisado for their helpful advice during the performance of this investigation.

Conflict of Interest

Neither of the authors from LDM Associates has received or will receive any compensation or monetary benefit from the publication of this article.

References

1. Lorrain P, Corson D (1970) Electromagnetic Fields and Waves. W.H. Freeman and Company.
2. Hjorth B (1980) Source Derivation Simplifies EEG Interpretation. American Journal of EEG Technology 20: 121-32.
3. Nunez PL (1981) Electric Fields of the Brain: Neuro-Physics of EEG. Oxford University Press.
4. Montgomery RW, Montgomery LD, Guisado R (1993) Electroencephalographic Scalp-Energy Analysis as a Tool for Investigation of Cognitive Performance. Biomedical Instrumentation &Technology 27(2): 137-142.
5. Montgomery LD, Montgomery RW, Guisado R (1995) Rheoencephalographic and Electroencephalographic Measures of Cognitive Workload: Analytical Procedures. Biological Psychology 40: 143-159.
6. Vailescu V, Margineanu GG (1982) Introduction to Neurobiophysics. Abacus Press, Kent.
7. Farrar D, Glauber R (1967) Multicollinearity in Regression Analysis: The Problem Revisited, Review of Economics and Statistics, February.
8. Montgomery LD, Gleason CR (1992) Simultaneous use of rheoencephalography and electroencephalography for the monitoring of cerebral function. Aviat Space Environ Med 63(4): 314-321.
9. Donchin E, Lindsley DB (1969) Averaged Evoked Potentials - Methods, Results, and Evaluation, US Government Printing Office, Washington DC.
10. Donchin E, W Ritter, C McCallum (1978) Cognitive Psychophysiology: The Endogenous Components of the ERP, in Callaway, E. et, al. (eds.) Event-Related Brain Potentials in Man, Academic Press, New York, pp. 349-412.
11. Thompson, W Lord Kelvin (1848) Note on the Integration of the Equations of Equilibrium of an Elastic Solid, Cambridge and Dublin Mathematical Journal 3: 87-9.
12. Hammond P (1981) Energy Methods in Electromagnetism. Clarendon Press: Oxford.
13. Maxwell JC (1891) Treatise on Electricity and Magnetism, Vol. I, Part 1, Chapter 4. Clarendon University Press, (reprinted by Dover Publications, New York, 1954)
14. Spehr W (1976) Source Derivation after Hjorth: An Improved EEG Derivation Technique. Electromedica, 4: 148-155.
15. Speckman EJ, Elger CE (1987) Introduction to the Neuropsychological Basis of the EEG and DC Potentials, pp. 1-13 in Niedermyer E, da Silva FlL (eds.) Electroencephalography: Basic Principles, Clinical Applications, and Related Fields, Second Edition, Urban and Schwarzenberg, Baltimore.
16. Vaughn HG, Arezzo J (1988) The Neural Basis of Event Related Potentials, Capter 3 in Pitcon, TW (ed.) Human Event Related Potentials: EEG Handbook (revised series, Vol3). Elsevier Science Publishing Co.
17. Gevins AS, Cutillo BA (1987) Signals and Cognition: Clinical Applications of Computer Analysis of EEG and other Neurological Signals Chapter 11 of Handbook of Electroencephalography and Clinical Neurophysiology, Revised Series Volume 2. Elsevier Science Publishers, New York, pp. 335-381.
18. Luria AR (1966) Higher cortical functions in man. Basic Books, New York.
19. Andreeva EK (1950) Disturbances of the System of Logical Associations in Frontal Lobe Lesions, Institute for Psychology, Moscow.
20. Filippycheva NA (1952) Inertia of the Higher Cortical Processes in Local Lesions of the Cerebral Hemispheres. USSR Academy of Medical Sciences, Moscow.
21. Maizel II (1959) Disturbance of Intellectual Activity Following Disintegration of Active Goal-Directed Activity. State University Press, Moscow.
22. Rao SM, Leo GJ, Bernardin L, Unverzagt F (May 1991) Cognitive Dysfunction in Multiple Sclerosis. I Frequency, Patterns, and Prediction. Neurology 41(5): 685-691.
23. Barber P (1988) Mental Workload, Attention and Performance, Chapter 4 in Applied Cognitive Psychology: An Information-Processing Framework, Methuen New York.
24. Bradshaw JL (1989) Hemispheric Specialization and Psychological Function, Wiley and Sons, New York.
25. Churchland PS (1986) Neurophilosophy, MIT Press, Cambridge.
26. Fisher FM (1966) The Identification Problem in Econometrics. McGraw-Hill, New York.
27. Gevins AS, Bressler SL, Cutillo BA, Illes J, Miller JC, et al. (1990) Effects of prolonged Mental Work on Functional Brain Topography, Electroencephalography and Clinical Neurophysiology 76: 339-350.
28. Gevins AS, Smith ME, Leong H, McEvoy L, Whitfield S, et al. (1998) Monitoring Working Memory Load during Computer-Based Tasks with EEG Pattern Recognition Methods. Human Factors 40(1): 79-91.

Gundel A, Wilson GF (1992) Topographical Changes in the Ongoing EEG Related to the Difficulty of Mental Tasks. Brain Topography 5(1): 17-25.

29. Hellige JB (ed.) (1983) Cerebral Hemisphere Asymmetry. Praeger, New York.
30. Homan RW (1987) The 10-20 Electrode System and Cerebral Location. American Journal of EEG Technology 28: 269-279.
31. Humphrey DL, Kramer AF (1994) Toward a Psychophysiological Assessment of Dynamic Changes in Mental Workload. Human Factors 36(1): 3-26.
32. Kramer AF, Trejo LJ, Humphrey D (1996) Psychophysiological Measures of Workload: Potential Applications to Adaptively Automated Systems. In R Parasuraman, J Mouloua (Eds.), Automation and Human Performance: Theory and Applications. Mahwah, NJ: Lawrence Erlbaum Associates, pp. 137-162.
33. Lorrain P, Corson D (1970) Electromagnetic Fields and Waves. W.H. Freeman and Company.
34. Lynn PA, Fruest W (1989) Digital Signal Processing with Computer Applications, Wiley & Sons.
35. Montgomery LD, Montgomery RW, Gerth WA, Guisado R (1990) Rheoencephalographic and electroencephalographic analysis of cognitive workload. Proceedings of the Third Annual IEEE symposium on Computer-Based Medical Systems, Chapel Hill, NC, June 3-6.
36. Montgomery RW, Montgomery LD, Guisado R (1992) Cortical localization of cognitive function by regression of performance on event related potentials. Aviat Space Environ Med 63(10): 919-924.
37. Nunez PL (1981) Electric Fields of the Brain: Neuro-Physics of EEG. Oxford University Press.
38. Papanicolaou AC, Johnstone J (1984) Probe Evoked Potentials: Theory, Method, and Applications. Intern J Neuroscience 24(2): 107-131.
39. Posner MI, Raichle ME (1994) Images of the Mind. WH Freeman and Company, New York.
40. Ruchkin DS (1987) Measurement of Event-Related Potentials: Signal Extraction in Pitcon TW (ed.): Handbook of Electroencephalography: Human Event Related Potentials. Elsevier Science Publishing Co.

41. Rudenck ZY (1953) Disturbance of Arithmetic Skill in Brain Lesions. USSR Academy of Medical Science, Moscow.

42. Trejo LJ, Shensa MJ (1999) Feature Extraction of Event-Related Potentials Using Wavelets: Application to Human Performance Monitoring. Brain and Language 66: 89-107.

43. Wang W, Begleiter H, Porjesz B (1994) Surface Energy, Its Density and Distance: New Measures with Application to Human Cerebral Potentials. Brain Topography 6(3): 193-202.

44. White EL (1989) Cortical Circuits: Synaptic Organization of the Cerbral Cortex; Structure, Function and Theory. Birkhauser, Boston.

45. Zhang XL, Begleiter H, Porjesz B, Wang W, Litke A (1995) Event Related Potentials During Object Recognition Tasks. Brain Research Bulletin 38(6): 531-538.